

Crystallization of poly(aryl ether ketone) polymers as revealed by time domain dielectric spectroscopy

T. A. Ezquerra*, F. Liu and R. H. Boyd

Department of Materials Science & Engineering, University of Utah, Salt Lake City, UT 84112, USA

and B. S. Hsiao

Central Research and Development, E.I. DuPont de Nemours, Experimental Station, Wilmington, DE 19880-0356, USA

(Received 21 November 1996; revised 13 January 1997)

Time domain dielectric methods have been used to compare the dynamics of the α relaxation of poly(aryl ether ketone) polymers. The real time variation of the macroscopic dielectric decay functions with crystallization time has been interpreted assuming an increase in the intermolecular cooperativity of the α relaxation as the polymer chains are obliged to move between crystalline regions. © 1997 Elsevier Science Ltd.

(Keywords: time domain dielectric relaxation; crystallization of poly(aryl ether ketone); frequency-time domain transformations)

INTRODUCTION

In most glass-forming liquids and polymers the relaxation of a measured property deviates from the linear exponential Debye behaviour characterized by a single relaxation time. In time domain, it has been shown that a good description of relaxation experiments can be achieved by means of the Kohlrausch–Williams–Watts (KWW) relaxation function¹

$$\phi(t) = \exp[-(t/\tau_{\text{kww}})^\beta] \quad (1)$$

where β takes values between 0 and 1. Here, τ_{kww} is a characteristic relaxation time and β characterizes the relaxation time distribution function. In particular, the time dependent dielectric constant exhibits a non-Debye behaviour which can be described by

$$\epsilon(t) = \epsilon_u + (\epsilon_r - \epsilon_u)[1 - \phi(t)] \quad (2)$$

where ϵ_r and ϵ_u are the relaxed ($t = \infty$) and unrelaxed ($t = 0$) dielectric constant values and $\phi(t)$ can be identified here with the macroscopic dielectric decay function. In the frequency domain, the dielectric complex permittivity $\epsilon^*(\omega)$ is related to $\phi(t)$ by a pure imaginary Laplace transformation^{1–3} of the form

$$\frac{\epsilon^*(\omega) - \epsilon_u}{\epsilon_r - \epsilon_u} = \int_0^\infty \exp(-i\omega t) \left[-\frac{d\phi(t)}{dt} \right] dt \quad (3)$$

The frequency dependence of the complex dielectric

permittivity can be phenomenologically described by the Havriliak–Negami (HN) function of the form⁴

$$\epsilon^*(\omega) = \epsilon_u + \frac{\epsilon_r - \epsilon_u}{[1 + (i\omega\tau_0)^b]^c} \quad (4)$$

where τ_0 is the central relaxation time of the relaxation time distribution function and b and c are shape parameters which describe the symmetric and the asymmetric broadening of the relaxation time distribution function, respectively⁴. The KWW stretched exponential describes with a single parameter, β , time domain experiments. There is considerable interest in the relation between the ‘ b ’ and ‘ c ’ parameters of the HN formulation, which describes a relaxation process in the frequency domain, and the corresponding β parameter which describes the same process in the time domain^{5–7}.

At temperatures above the glass transition temperature (T_g), molecular motions in polymers and glass formers are typically extended to several molecular segments and give rise to the appearance of the α relaxation. Some polymers may partially crystallize provided they are heated at temperatures above T_g rendering to semicrystalline systems. In semicrystalline polymers, at $T > T_g$, the polymer chains remaining in the amorphous phase are restricted to move between the crystalline regions^{2,8–10}. This chain confinement modifies the dynamics of the α relaxation process producing a slowing down of the molecular motions and a broadening of the relaxation time distribution function as the main features^{2,11–13}.

Until now the majority of studies related to crystallization and dielectric relaxation have been carried

* To whom correspondence should be addressed at: Instituto de Estructura de la Materia, C.S.I.C. Serrano 119, Madrid 28006, Spain

out and analysed in the frequency domain^{2,11,12,14,15}. Frequency domain methods have been shown to be very useful to characterize dielectrically crystallization processes in real time^{13,16,17}. Normalized macroscopic dielectric decay functions can be computed by inverse Laplace transformation of experimental data^{5,13,15}. An appealing practical feature of the direct time domain method in real time crystallization studies is that the measuring time is well defined in comparison with the time scale of the crystallization. That is, the dielectric time trace is repeatedly captured over the same fixed time interval as crystallization proceeds. It is thus especially apparent whether the measuring interval is small compared with property evolution due to crystallization.

In the present paper we have studied in time domain the dielectric behaviour of two initially glassy polymers of the poly(aryl ether ketone) family: poly(aryl ether ketone ketone) (PEKK) and poly(aryl ether ether ketone) (PEEK). The aim of the work is twofold. On one hand, it is to establish, from the evolution of the measured dielectric decay functions, a relationship between the change of the shape parameters and the restriction on

the overall chain mobility imposed by crystallization. On the other hand, a first attempt has been made to use time domain dielectric spectroscopy to perform real time crystallization measurements in polymeric materials.

EXPERIMENTAL

Poly(aryl ether ketone ketone) (PEKK) and poly(aryl ether ether ketone) (PEEK) are semirigid polymers from the poly(aryl ether ketone) group. PEKK can be prepared from diphenyl ether, terephthalic acid (T) and isophthalic acid (I). By controlling the amount of T and I components, polymers with different *para/meta* phenyl isomer ratios can be prepared. In the present work we investigated a 60/40 PEKK specimen, synthesized at DuPont, with $T_g = 155^\circ\text{C}$, $M_n \approx 30\,000\text{ g mol}^{-1}$ and $M_w \approx 100\,000\text{ g mol}^{-1}$ (ref. 18). PEEK was obtained from ICI (450 G) with $T_g = 145^\circ\text{C}$, $M_n \approx 12\,500\text{ g mol}^{-1}$ and $M_w \approx 40\,000\text{ g mol}^{-1}$. The starting samples were amorphous films with a thickness of about 0.005 cm. Time domain measurements of the dielectric constant were accomplished in a range of $10^{-6} < t < 10^1$ s by using

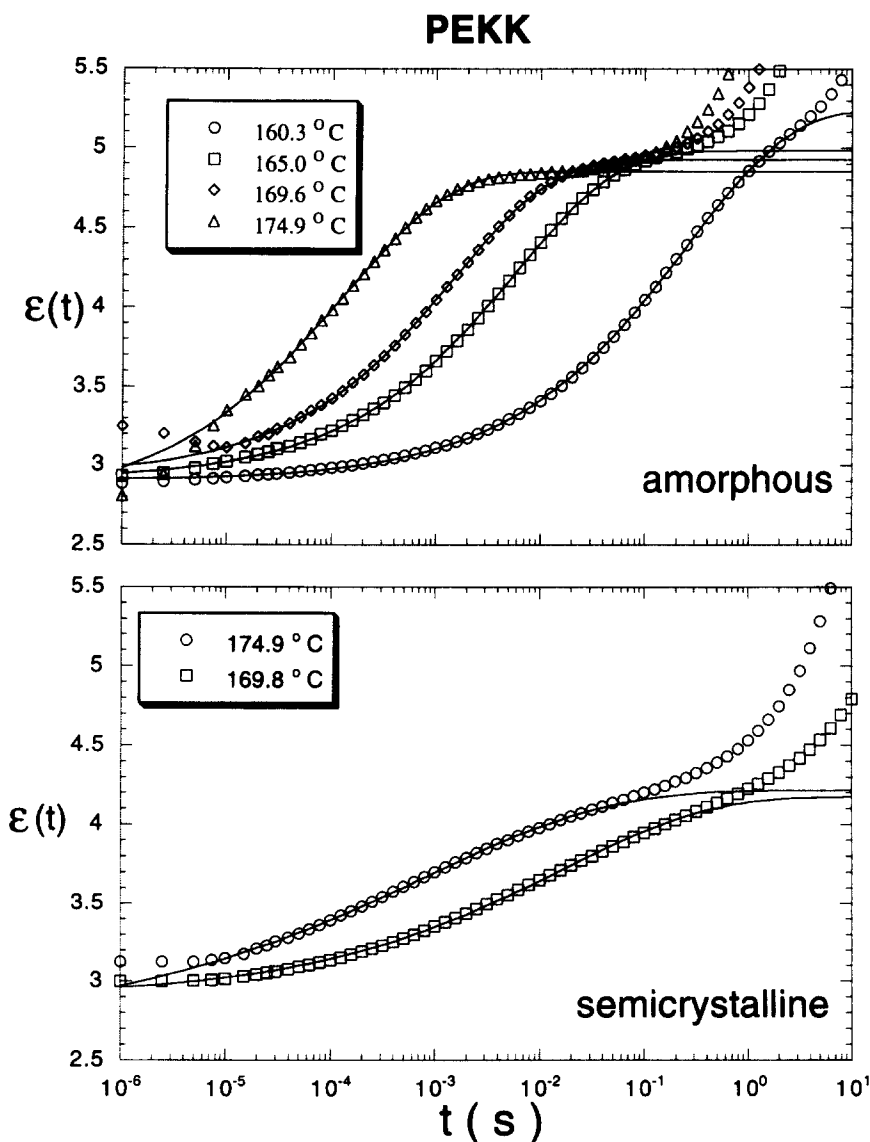


Figure 1 Dielectric constant, $\epsilon(t)$, for the amorphous (upper) and semicrystalline (lower) PEKK sample as a function of time for different temperatures labelled in the inset. The continuous lines are fits according to equations (1) and (2). Parameters of the fits are shown in Table 1

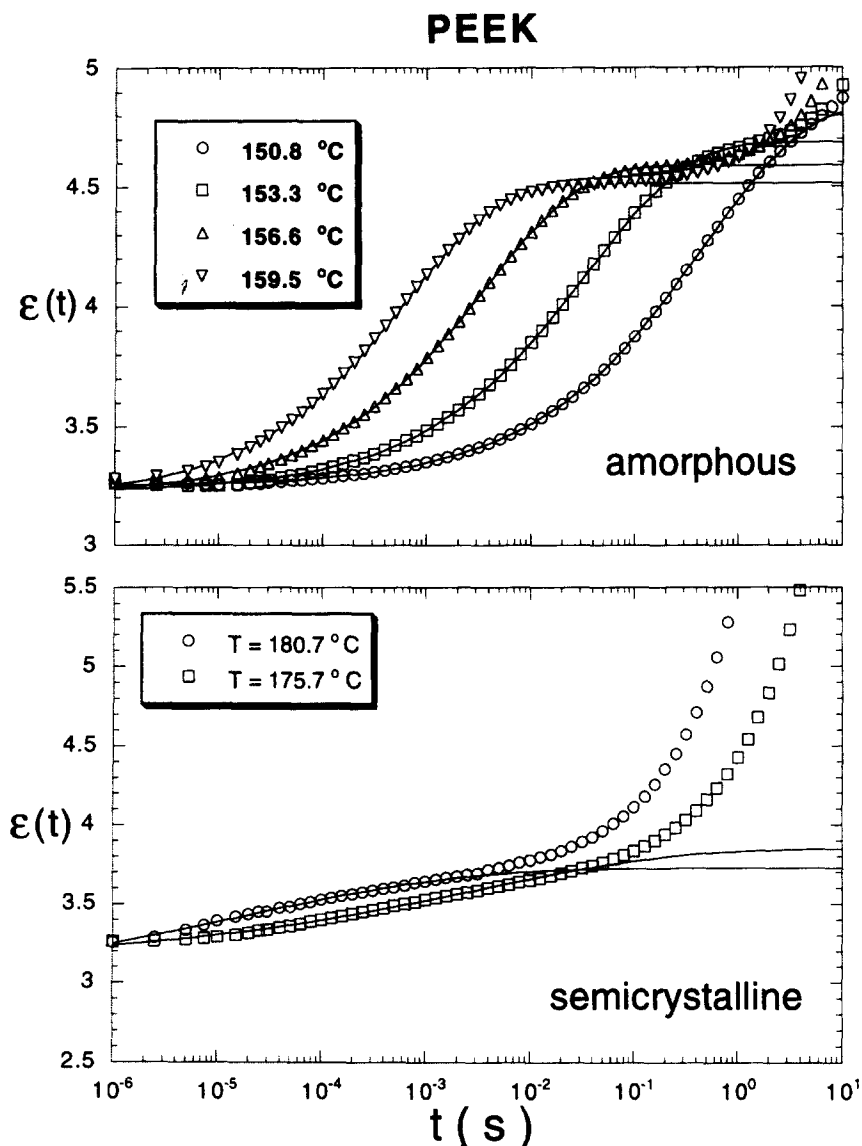


Figure 2 Dielectric constant, $\epsilon(t)$, for the amorphous (upper) and semicrystalline (lower) PEEK sample as a function of time for different temperatures labelled in the inset. The continuous lines are fits according to equations (1) and (2). Parameters of the fits are shown in *Table 2*

a dielectric spectrometer based on the design of Mopsik¹⁹ and manufactured by IMASS Corp., Hingham, MA. Accurate time to frequency data transformation can be done allowing a frequency domain ranging from 10^{-3} Hz to 10^4 Hz routinely available. Films with a three terminal connection consisting of an inner circular electrode (1 cm diameter) and an outer guard ring were prepared by sputtering gold in both free surfaces. The error of the absolute accuracy of the $\epsilon(t)$ values can be estimated to be below 10%. The specimens were placed between two copper electrodes and the dielectric cell was introduced in a temperature controlled furnace. To perform isothermal crystallization measurements in real time the sample was brought to the crystallization temperature at a constant heating rate of $0.6^\circ\text{C min}^{-1}$. After reaching the selected T_c , $\epsilon(t)$ measurements were performed as a function of crystallization time. Each measurement required about 10 s. The experimental conditions were carefully chosen to both avoid significant precrystallization of the sample during the heating process and to place the α relaxation process in the middle of our experimental time domain window.

RESULTS

Time domain dielectric relaxation of the glassy and semicrystalline polymers

Dielectric constant, $\epsilon(t)$, data measured for the initially amorphous PEKK and PEEK samples at different temperatures are shown in the upper *Figures 1* and *2* respectively. In this temperature range a main dielectric process, α , is clearly distinguished by the measured sigmoidal-like increase of $\epsilon(t)$ with time. The ultimate increase of $\epsilon(t)$ observed typically for times $t > 10^{-1}$ s is characteristic of an additional conduction process. The dielectric curves shift towards shorter times as temperature increases.

Crystallization of the initially amorphous samples was achieved by holding the samples at a given temperature ($T_c = 188^\circ\text{C}$ for PEKK and $T_c = 160^\circ\text{C}$ for PEEK) during more than 3 h and subsequent slow cooling down to room temperature. Under these conditions it has been previously shown that both polymers develop a crystallinity of about 20%^{13,14}. For the semicrystalline specimens (lower *Figures 1* and *2*) the $\epsilon(t)$ data exhibit a conspicuous reduction in the intensity of the relaxation.

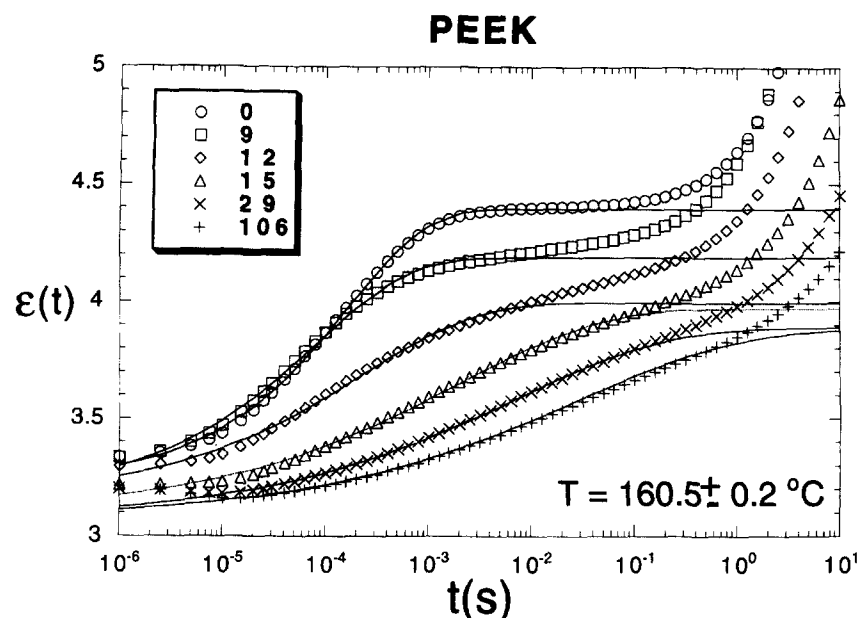


Figure 3 Real time evolution of the α relaxation dielectric constant, $\epsilon(t)$, values vs. time during an isothermal crystallization process at $T = 160.5 \pm 0.2^\circ\text{C}$ at selected crystallization times shown in the inset. The continuous lines are fits according to equations (1) and (2). Fitting parameters are shown in *Figure 4*

Table 1 T ($^\circ\text{C}$), $\Delta\epsilon$, ϵ_u , τ_{kww} and β obtained from the fitting of equations (1) and (2) for the α relaxation data of the amorphous samples

PEKK T ($^\circ\text{C}$)	$\Delta\epsilon$	ϵ_u	τ_{kww} (s)	β	PEEK T ($^\circ\text{C}$)	$\Delta\epsilon$	ϵ_u	τ_{kww} (s)	β
160.3	2.34	2.9	2.5×10^{-1}	0.43	150.8	1.59	3.24	4.8×10^{-1}	0.44
165	2.07	2.9	5.6×10^{-3}	0.44	153.3	1.46	3.22	3.6×10^{-2}	0.45
169.6	2	2.92	1.5×10^{-3}	0.46	156.6	1.37	3.2	3.6×10^{-3}	0.47
174.9	2.12	2.72	1.3×10^{-4}	0.42	159.5	1.31	3.19	6.4×10^{-4}	0.48

Table 2 T ($^\circ\text{C}$), $\Delta\epsilon$, ϵ_u , τ_{kww} and β obtained from the fitting of equations (1) and (2) for the α relaxation data of the semicrystalline samples

PEKK T ($^\circ\text{C}$)	$\Delta\epsilon$	ϵ_u	τ_{kww} (s)	β	PEEK T ($^\circ\text{C}$)	$\Delta\epsilon$	ϵ_u	τ_{kww} (s)	β
169.8	1.14	2.91	9.5×10^{-3}	0.33	175.7	0.72	3.12	2.8×10^{-3}	0.22
174.9	1.52	2.7	7.4×10^{-4}	0.24	180.7	0.84	2.87	1.6×10^{-5}	0.2

Real time variation of the α relaxation process upon crystallization

Real time crystallization experiments by frequency domain dielectric methods have been previously performed in PEKK polymers^{13,20}. It was shown that in the temperature range at which real time measurements become meaningful, the frequency of maximum loss of the α relaxation process occurs above 10^4 Hz. In time domain, this implies that most of the information about the relaxation process occurs at times $t < 10^{-3}$ s. This fact makes PEKK not very suitable for a real time crystallization experiment by time domain methods. On the contrary, PEEK shows faster kinetics of crystallization in comparison to PEKK¹⁸ while the relaxation process remains in the middle of our accessible experimental time window. *Figure 3* shows the real time evolution of $\epsilon(t)$ for the α relaxation during an isothermal crystallization process at $T_c = 160.5 \pm 0.2^\circ\text{C}$ in PEEK. Each curve represents the dependence of $\epsilon(t)$ vs. time at a selected crystallization time labelled in the inset of the figure. The initial curve, at $t = 0$, corresponds to the initially amorphous polymer. As crystallization

proceeds two main features are observed in *Figure 3*. Firstly, there is a reduction in the intensity of the measured step in $\epsilon(t)$ as the crystallization time increases. Secondly, a displacement of the curves towards longer time values is observed.

Phenomenological analysis of the experimental results

The continuous lines represented in *Figures 1, 2* and *3* correspond to fittings calculated according to equations (1) and (2). A subroutine based on the Newton method²¹ was used in the fitting. The appearance of Maxwell–Wagner–Sillars polarization is apparent as upturns in the dielectric constant at longer times. No attempt was made to model or fit this behaviour. The parameters calculated in these fittings including β , $\Delta\epsilon$ and τ_{kww} are presented in *Tables 1* and *2* for the temperature evolution of $\epsilon(t)$ in PEKK and PEEK (*Figures 1* and *2*). For the real time crystallization experiment performed in PEEK (*Figure 3*) the calculated parameters are represented in *Figure 4* as a function of crystallization time. From the presented results some interesting features can be identified as crystallization proceeds. Firstly, a reduction

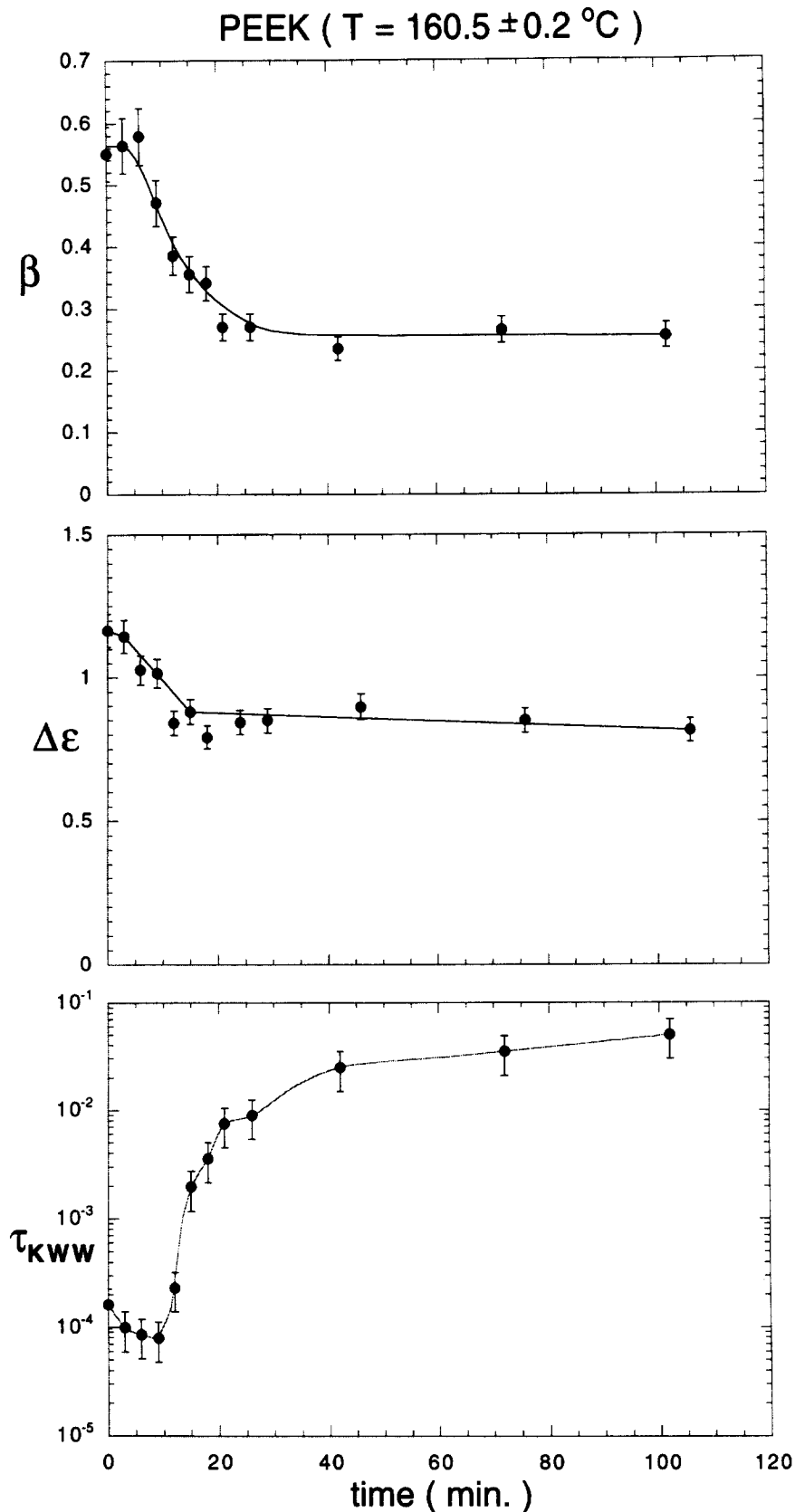


Figure 4 Real time evolution of β , $\Delta\epsilon$, and τ_{kww} during the isothermal crystallization process. Continuous lines are a guide to the eye

of both the stretched exponential, β , and of the dielectric strength, $\Delta\epsilon$, which decrease at earlier stages of crystallization and level off for longer crystallization times. Secondly, an increase of the characteristic relaxation time τ_{kww} which finally levels off as crystallization time increases. $\epsilon^*(\omega)$ data for the amorphous and

semicrystalline samples were numerically obtained by a Laplace transformation¹⁹ of the time domain $\epsilon(t)$ values. The $\epsilon''(\omega)$ results are represented vs. $\epsilon'(\omega)$ as Argand plots in *Figures 5* and *6* for the amorphous and semicrystalline PEKK and PEEK samples respectively. The continuous lines represent the best fit of the obtained

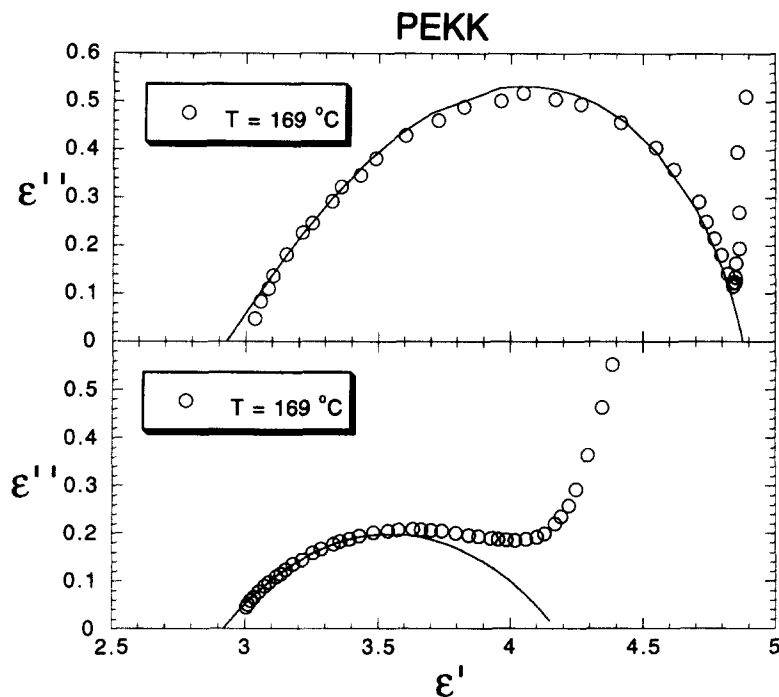


Figure 5 Argand plots of the α relaxation for amorphous (upper) and semicrystalline (lower) PEKK. Solid curves denote best fits calculated according to equation (4). Parameters of the fits are shown in Table 3

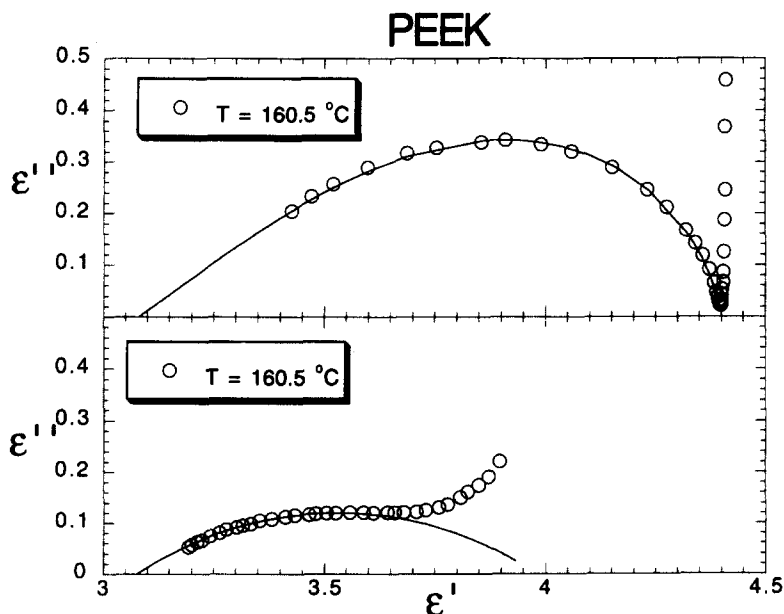


Figure 6 Argand plots of the α relaxation for amorphous (upper) and semicrystalline (lower) PEEK. Solid curves denote best fits calculated according to equation (4). Parameters of the fits are shown in Table 4

Table 3 $\Delta\epsilon$, b , c and τ_0 obtained from the fitting of equation (4) for the PEKK α relaxation data shown in Figure 5

PEKK	$\Delta\epsilon$	b	c	τ_0 (s)
Amorphous	1.95	0.77	0.57	3.8×10^{-3}
Semicryst.	1.26	0.39	1	9.2×10^{-3}

Table 4 $\Delta\epsilon$, b , c and τ_0 obtained from the fitting of equation (4) for the PEEK α relaxation data shown in Figure 6

PEEK	$\Delta\epsilon$	b	c	τ_0 (s)
Amorphous	1.32	0.85	0.41	4.7×10^{-4}
Semicryst.	0.9	0.33	1	3.1×10^{-2}

values by the Havriliak–Negami function [equation (4)]. The corresponding fitting parameters are shown in Tables 3 and 4. From the present results it follows that in addition to the decrease of the relaxation strength $\Delta\epsilon$, the relaxation curves broaden and become symmetric for the semicrystalline samples.

DISCUSSION

The present experiments show that the macroscopic dielectric decay function is severely affected by the crystallization process. The experimental data can be well described by means of the KWW function. The sigmoidal-shape variation of the magnitudes presented

in Figure 4 seems to follow the characteristic features of an isothermal crystallization process. The observed evolution of the α relaxation process in real time, as analysed by equations (1) and (2), reflects a variation of the time distribution function during the isothermal crystallization. Since $\Delta\epsilon$ is proportional to the density of dipoles involved in the α -relaxation²², the decrease of $\Delta\epsilon$ with crystallization time can be associated with the progressive reduction of the amorphous phase as the polymer crystallizes, which results in more and more of the polymer chain segments being immobilized within the crystalline phase. The observed increase of the characteristic relaxation time, τ_{KWW} , with crystallization time indicates a progressive reduction of overall mobility of the polymeric chains as the system is filled with crystals. As crystallinity develops the distribution of relaxation times becomes broader as revealed by the decrease of β . As the system crystallizes the α relaxation process is increasingly restricted to the interlamellar amorphous regions. In addition, segments of the polymeric chains included in the crystals can hinder the overall mobility of bonded segments which remain in the amorphous phase by restricting the available possible conformations¹¹. The above described results are in qualitative agreement with previous measurements performed in PEKK by frequency domain methods¹³.

In the time domain, the model²³ proposed by Ngai *et al.* to explain the physical basis of the KWW stretched exponential considers the coupling of relaxing species with neighbouring non-bonded ones as the main reason for non-Debye behaviour. This intermolecular coupling or degree of cooperative provokes a slowing down of the segmental relaxation giving rise to a KWW decay function. The degree of coupling is characterized by a new parameter n related to the stretching exponential by $\beta = 1 - n$. According to this model, a decrease of $\beta = 1 - n$ is expected provided that a strengthening of the intermolecular coupling between the relaxing species occurs. Intrachain coupling provoking restrictions of conformational transitions may also increase the intermolecular cooperativity²⁴. For semicrystalline polymers the interconnection of chain segments in the amorphous phase to the crystals increase the cooperativity of these segments by reducing the number of conformations¹¹. Consequently, the differences in β observed for the amorphous and the semicrystalline samples can be interpreted as due to an increase of interchain coupling between the relaxing units caused by the additional intrachain constraints introduced by the crystallinity.

In the frequency domain, Schönhals and Schlosser have proposed a model for the molecular dynamics above the glass transition in which the HN b parameter can be related to the large scale motions while the $b \cdot c$ product to the small scale ones²⁵. Experimental support of the model has been provided by different dielectric techniques²⁶. The observed variation of the b and c parameters upon comparing amorphous and semicrystalline samples (Figures 5 and 6) is in good accordance with the predictions of this model. The decrease of b could be interpreted in terms of the increasing hindrance of large scale motions when crystals are present. There is not very much difference in the $b \cdot c$ value in the amorphous and the semicrystalline specimens suggesting that the small scale motions are less affected by the crystallinity. The extension of these studies covering

other polymeric systems can probably help to explain the physical mechanisms controlling the α relaxation of the confined amorphous phase in semicrystalline polymers.

CONCLUSIONS

Time domain dielectric methods can be used to follow changes appearing in glassy polymers during isothermal crystallization in real time. As in previous experiments performed in the frequency domain, the variation of the dielectric parameters follow a sigmoidal-shaped evolution characteristic of isothermal crystallization processes in polymeric materials. The macroscopic dielectric decay functions can be well described assuming a KWW shape. The characteristic relaxation time increases with crystallization time suggesting a progressive reduction of overall mobility of the polymeric chains as the system becomes more crystalline. Concurrently, an increase of the stretching of the KWW function is detected which can be qualitatively interpreted as due to an increase of the interchain coupling between the relaxing species in the amorphous phase.

ACKNOWLEDGEMENTS

T.A.E. is indebted to the DGICYES (Spain) for the tenure of a sabbatical fellowship. Partial financial support was provided by DGICYT (Grant No. PB 94-0049) Spain and NEDO's International Joint Research Program, Japan. This work was also supported by the Polymer Program, Division of Materials Research, National Science Foundation (USA).

REFERENCES

- Williams, G. and Watts, D. C., *Trans. Faraday Soc.*, 1970, **66**, 80.
- Williams, G., *Adv. Polym. Sci.*, 1979, **33**, 59.
- Cook, M., Watts, D. C. and Williams, G., *Trans. Faraday Soc.*, 1970, **66**, 2503.
- Havriliak, S. and Negami, S., *Polymer*, 1967, **8**, 161.
- Boese, D., Momper, B., Meier, G., Kremer, F., Hagenah, J. U. and Fischer, E. W., *Macromolecules*, 1989, **22**(12), 4416.
- Alvarez, F., Alegria, A. and Colmenero, J., *Phys. Rev. B*, 1993, **47**, 125.
- Havriliak, S. and Havriliak, S. J., *Polymer*, 1996, **37**, 4107.
- Boyd, R. H., *Polymer*, 1985, **26**, 323.
- Sauer, B. B. and Hsiao, B. S., *Polymer*, 1995, **36**, 2553.
- Verma, R. K. and Hsiao, B. S., *Trends in Polym. Sci.*, 1996, **4**(9), 312.
- Coburn, J. C. and Boyd, R. H., *Macromolecules*, 1986, **19**, 2238.
- Schönhals, A. and Schlosser, E., *Colloid & Polym. Sci.*, 1989, **267**, 963.
- Ezquerro, T. A., Majszczyk, J., Baltá-Calleja, F. J., López-Cabarcos, E., Gardner, K. H. and Hsiao, B. S., *Phys. Rev. B*, 1994, **50**, 6023.
- Jonas, A. and Legras, R., *Macromolecules*, 1993, **26**, 813.
- Fukao, K. and Miyamoto, Y., *Polymer*, 1993, **34**, 238.
- Ezquerro, T. A., Roslaniec, Z., López-Cabarcos, E. and Baltá-Calleja, F. J., *Macromolecules*, 1995, **28**, 4518.
- Ezquerro, T. A., Baltá-Calleja, F. J. and Zachmann, H. G., *Polymer*, 1994, **35**, 2600.
- Gardner, K. H., Hsiao, B. S., Matheson, R. R. Jr. and Wood, B. A., *Polymer*, 1992, **33**, 2483.
- Mopsik, F. I., *Rev. Sci. Instr.*, 1984, **55**, 79.
- Ezquerro, T. A., Majszczyk, J., Baltá-Calleja, F. J., López-Cabarcos, E., Gardner, K. H. and Hsiao, B. S., *Physica Scripta*, 1994, **T55**, 212.

21. Ebert, K., Ederer, H. and Isenhour, T. L., *Computer Applications in Chemistry*. VCH, Weinheim, 1989.
22. Hedvig, P., *Dielectric Spectroscopy of Polymers*. Adam Hilger Ltd, Bristol, 1977.
23. Ngai, K. L., Rajagopal, A. K. and Teiler, S., *J. Chem. Phys.*, 1988, **88**(8), 5086.
24. Ngai, K. L. and Roland, C. M., *Macromolecules*, 1993, **26**, 6824.
25. Schönhals, A. and Schlosser, E., *Colloid & Polym. Sci.*, 1989, **267**, 125.
26. Schönhals, A., Kremer, F. and Schlosser, E., *Phys. Rev. Lett.*, 1991, **67**, 999.